

Cite this: *Food Funct.*, 2023, **14**, 1773

Modification of the functional properties of chickpea proteins by ultrasonication treatment and alleviation of malnutrition in rat

 Yue Gao,^{†a} Xiyu Hao,^{†b} Yichen Hu,^{†c} Nong Zhou,^d Qiang Ma,^{*e} Liang Zou^c and Yang Yao^{*a,f}

High-intensity ultrasonication (HIU) is an emerging technology for improving the functional properties of the leguminous proteins in the food industry. In this study, chickpea protein (CP) was treated at 150 W for 30 min to obtain ultrasonic chickpea protein (UCP). The physicochemical (particle size, ζ -potential, hydrophobicity, and free sulfhydryl) and structural properties (FTIR) were changed after the HIU treatment, which led to an improvement of functional properties, including the solubility, emulsifying, and foamability in UCP. The chickpea protein diet (CPD) and ultrasound chickpea protein diet (UCPD) were supplemented to undernourished weaning rats to assess their potential in improving malnutrition. After 6 weeks of administration, the body weight of malnourished rats in UCPD increased by 11.97% compared with that in CPD. The results in OMICS showed that beneficial bacteria and short-chain fatty acids were positively related to growth. This work demonstrated the physicochemical and functional properties of CP and UCP and guided the application of the UCP to malnutrition improvement.

Received 24th August 2022,
Accepted 9th January 2023

DOI: 10.1039/d2fo02492f

rsc.li/food-function

1. Introduction

COVID-19 pandemic has been undermining nutrition worldwide in recent years, leading to a surge in child malnutrition.¹ In low- and middle-income countries, where protein sources are scarce, the use of agricultural crops, particularly legumes, as a source of micronutrients and macronutrients is a promising approach. Chickpea, as one of the most consumed legumes worldwide, represents nearly 20% of production in

the global legume. It is known for its higher protein content and well-balanced amino acids.^{2,3} Therefore, chickpea protein (CP) is a greatly valuable protein emerging to be utilized widely. However, the application of leguminous proteins has been limited by its unsatisfactory functional properties (poor solubility, lower emulsifying, and foamability). Thus, appropriate technologies need to be implemented to improve the functional properties of leguminous protein for its wide range of use.

It is well known that the functional properties of leguminous proteins depend on their physicochemical properties.⁴ Ultrasound, as an environmentally sustainable technology, has become the first choice to modify physicochemical and functional properties in leguminous protein.⁵ Scientists uncovered that high-intensity ultrasonication (HIU) modulated the physicochemical properties (particle size, sulfhydryl content, and hydrophobicity) in soy protein, and subsequently improved their functional features such as solubility.⁶ In addition, hydrophobicity and particle size were positively influenced by HIU treatment in pea and black soybean protein isolates in which a more soluble protein solution was observed.^{7,8} Moreover, the change in structure by HIU induced the unfolding and breaking of soy protein and pea protein, which gave more opportunities for the protein to fully cover emulsion droplets and simultaneously increased the emulsifying.⁹ The higher hydrophobicity and lower particle size in soy protein after the HIU treatment increased the contact opportunity and interaction between water and protein, thus the foamability

^aInstitute of Crop Science, Chinese Academy of Agricultural Sciences, No. 12 Zhongguancun South Street, Haidian District, Beijing, 100081, People's Republic of China. E-mail: yaoyang@caas.cn

^bHeilongjiang Feihe Dairy Co., Ltd., C-16, 10A Jiuxianqiao Rd, Chaoyang District, Beijing, 100015, People's Republic of China

^cKey Laboratory of Coarse Cereal Processing, Ministry of Agriculture and Rural Affairs, Sichuan Engineering & Technology Research Center of Coarse Cereal Industrialization, School of Food and Biological Engineering, Chengdu University, Chengdu, Sichuan, 610106, People's Republic of China

^dLaboratory for Green Cultivation and Deep Processing of Three Gorges Reservoir Area's Medicinal Herbs, College of Life Science & Engineering, The Chongqing Engineering, Chongqing Three Gorges University, Chongqing, 404000, People's Republic of China

^eDepartment of Basic Medicine, Chongqing Three Gorges Medical College, Chongqing, 404120, People's Republic of China. E-mail: maqiang@cqgtg.edu

^fKey Laboratory of Grain Crop Genetic Resources Evaluation and Utilization, Ministry of Agriculture and Rural Affairs, Institute of Crop Sciences, Chinese Academy of Agricultural Sciences, No. 12 Zhongguancun South Street, Haidian District, Beijing, 100081, People's Republic of China

[†]These authors contributed equally to this work.



improved.¹⁰ Except for the extraordinary effects in shaping physicochemical properties in leguminous protein, recently researchers uncovered that more amino acids were exposed and stable when leguminous proteins were treated with HIU.^{5,11} Meanwhile, amino acids are supplementarily related to the improvement of growth in undernourished rats. Therefore, performed ultrasonication potentially promoted CP utilization by modulating the physicochemical and functional properties and provided new insight into attenuating malnutrition with leguminous proteins. However, there are limited studies that have compared the difference between CP and ultrasound chickpea protein (UCP) in its physicochemical, structural, and functional properties and alleviating undernutrition effects *in vivo*.

Hence, this work aimed to (i) compare the changes of CP and UCP in physicochemical, structural, and functional properties (ii) evaluate the potential effect on a malnourished model of rats supplemented with different diets (chickpea protein diet (CPD) and the ultrasound chickpea protein diet (UCPD)).

2. Materials and methods

2.1. Materials and reagents

The CP powder (purity $\geq 95\%$) was provided by Gushen Biological Technology Group Co., Ltd (Yantai, China) and extracted following their protocol (alkaline extraction followed by isoelectric precipitation). The E.N.Z.A.® Stool DNA isolation kits were provided by Omega Bio-Tek Inc. (Norcross, USA). Angiotensin-converting enzyme 2 (ACE 2) and IGF-1 ELISA kits were obtained from Biorbyt (Princeton, USA) and Abcam (Cambridge, UK), respectively. All the other chemicals were all analytical reagents.

2.2. Ultrasound treatment

CP (100 g) was dispersed in 1 L deionized water and subsequently stirred for 1 h (room temperature), then, the solution was treated with an ultrasonic processor (Bandelin Sonopuls HD3200, Berlin, Germany). The TT 13/FZ probe was submerged at 2 cm depth and the ultrasonic power was 150 W for 30 min (pulse on 2 s and off 2 s). After the solution was dried using a vacuum freeze dryer, the UCP was obtained.

2.3. Physicochemical and functional properties

2.3.1. Particle size and ζ -potential analysis. The particle size and ζ -potential of samples (1 mg mL⁻¹ in 10 mM phosphate buffer) were measured using the Zetasizer Nano ZS (Malvern Instruments Ltd, Worcestershire, UK) instrument. Samples were centrifuged at 10 000g for 10 min before being filtered through a 0.45 μ m size membrane to filter out insoluble elements. Then samples were transferred to a cubic cuvette to be tested for particle size using the Zetasizer Nano-ZS equipment. The other batch of samples was placed into a capillary cell containing electrodes to determine the electrophoretic mobility of the particles, which were then converted

to ζ -potential values using the Smoluchowski mathematical model.

2.3.2. Micro-structure of the mixture. A confocal laser scanning microscope 980 (CLSM, Carl Zeiss AG, Jena, Germany) was used to observe the micro-structure of CP and UCP. This method was described in a previous report.¹² Diluted in dimethylformamide, rhodamine B (0.1% w/v) was used to label the protein. After the samples were diluted by deionized water to 14 mg mL⁻¹, 20 μ L rhodamine B was added into the solution for 15 min in the dark. Finally, the micro-structure of the solution was observed by CLSM.

2.3.3. Transmission electron microscopy (TEM). The morphology of the samples was observed through a transmission electron microscope (Hitachi HT7700) at 80 kV acceleration voltage. A one-drop sample is laid on a carbon-coated copper grid, dyed with phosphotungstic acid for 3 minutes, then air dried for 10 minutes before finally imaging.

2.3.4. Hydrophobicity. The hydrophobicity of the sample was determined as discussed in a previous study¹³ with some modifications. A series of protein solutions with concentrations from 0.002 to 0.01% was prepared at pH 3.0, 5.0, 7.0, and 9.0. 20 μ L of the ANS solution (8.0 mM) was added to 4 mL of diluted protein solution and mixed for 10 s.

Briefly, the samples were diluted with the phosphate buffer of different pH values (pH 3.0, 5.0, 7.0, and 9.0). Twenty microliters of ANS-Na (8 mM in 0.1 M phosphate buffer (pH 7.0)) were added to 4 mL of different concentration sample solutions, respectively, and subsequently, the mixture was incubated for 15 min in the dark. Two hundred microliters of the sample were placed in 96-well plates to detect the fluorescence intensity (FI) in an F2500 fluorescence spectrometer (PerkinElmer, Waltham, USA), in which the excitation and absorption wavelengths were 390 nm and 470 nm, respectively. Meanwhile, the same volume of ANS + 0.1 M phosphate buffer was measured as blank. The hydrophobicity was calculated by FI/(protein concentration).

2.3.5. The free sulfhydryl content (FSC) analysis. The FSC was measured according to the description by Hu *et al.*¹⁴ Briefly, one milliliter of each sample (1 mg mL⁻¹) was diluted in 3 mL buffer (0.086 M Tris, 0.09 M glycine, 4.0 mM dinitrofluorobenzene (DNTB), pH 8). Forty microliters of DNTB (4 mg mL⁻¹ in buffer) were added to the supernatant, which was separated from the prepared sample (10 000g, 15 min). The mixture was kept at 25 °C for 20 min and the absorbance was measured at 412 nm, and was named A₁ (Molecular Devices, San Jose, USA). The solubilizing buffer was used as the reagent blank. The solubilizing buffer (50 μ L) was used instead of the DNTB reagent solution as the protein blank named A₂. The FSC was calculated as follows:

$$\text{FSC} (\mu\text{mol g}^{-1} \text{protein}) = \frac{(75.53 \times D \times A)}{C} \quad (1)$$

where D is the dilution ratio, and $A = A_1 - A_2$.

2.3.6. Solubility analysis. The solubilities of CP and UCP in different pH (pH 3.0, 5.0, 7.0, and 9.0) were determined according to a previous method.¹⁵ After centrifugation (6000g,



15 min) (1%, w/w), one milliliter of the sample supernatant was mixed with 4 mL of biuret reagent. The absorbance was determined at 540 nm after it was incubated for 30 min in the dark. Casein was used as the standard. Solubilities were calculated from the percentage of the primary protein present in the supernatant.

2.3.7. Emulsion capacity analysis. The emulsion capacity was measured based on a modified previous study.¹⁶ The mixture (1 mg mL⁻¹) was added with soy oil (1:10, v/v) with pHs adjusted to 3.0, 5.0, 7.0, and 9.0. A high-speed homogenizer TUOHE 500 (Shanghai, China) was used to mix the solution completely (12 000 rpm, 2 min). Then, the emulsion (1 mL) at the bottom was immediately mixed with 0.1% sodium dodecyl sulfate (10 mL). The absorbance at 0 min (A_0) and 10 min (A_{10}) was recorded at 500 nm (Molecular Devices, San Jose, USA). Finally, the emulsion activity (EAI) and the emulsion stability (ESI) were obtained as follows:

$$\text{EAI} = \frac{2 \times 2.303 \times A_0 \times D}{C \times (1 - \alpha) \times 10^4} \quad (2)$$

$$\text{ESI} = \frac{A_0}{A_0 - A_{10}} \quad (3)$$

where C is the concentration of the sample and D is the dilution factor, α is the volume of oil in the solution.

2.3.8. Foaming ability (FA) and foam stability (FS) analysis. The FA and FS of samples were measured according to a previous report with some modifications.¹⁰ The sample solution (5%, 15 mL) with pHs adjusted to pH 3.0, 5.0, 7.0, and 9.0 were homogenized for 2 min at a speed of 8000g and moved to a measuring cylinder immediately. The volume of the foam was measured at 0 min and at 90 min, which is recorded as V_0 and V_{90} , respectively.

$$\text{FA}\% = \frac{V_0}{15} \times 100 \quad (4)$$

$$\text{FC}\% = \frac{V_0}{V_{90}} \times 100 \quad (5)$$

2.3.9. The FT-IR. The sample was scanned in the absorbance mode from 4000 to 400 cm⁻¹ with a resolution of 4 cm⁻¹ at 64 scans using an FT-IR spectrophotometer (Bruker, Rosenheim, Germany). The background was collected before each sample scanning.

2.4. Malnutrition evaluation

2.4.1. Animal study. The undernutrition study *in vivo* was conducted as that described in a previous study.¹⁷ Thirty male weaning Sprague-Dawley (SD) rats, supplied by the Vital River Laboratory Animal Technology Co. Ltd (Beijing, China), were acclimatized for one week in the laboratory. Rats were firstly fed with 7% protein to induce an undernourished model (weight decreased by 43.58% ± 2.39 after 3 weeks) before being divided into 3 groups of ten rats each as follows: low (7%) casein group (LG), chickpea protein diet (CPD) and ultrasound chickpea protein diet (UCPD). Rats in

each group were fed with corresponding diets (Xietong Pharmaceutical Bio-Engineering Co., Ltd, Nanjing, China). The experimental animals were weighed, and their tail length was monitored each week. The diet composition in each group is shown in Table 1. Throughout the experiment, all rats were kept in a standard animal house at 24 °C with free access to water and food. On day 54, the overnight fasted rats were euthanized after isoflurane anesthesia. The serum was prepared immediately from blood drawn from the inferior vena cava. IGF-1 and ACE 2 levels in the serum were quantified using ELISA kits. The colonic contents were also collected. For analysis, all samples were kept at -80 °C after freezing in liquid nitrogen until analysis was performed. The animal experiments were performed by the Pony Testing International Group (Animal Care and Use SYXK (Beijing) 2018-0022).

2.4.2. Short-chain fatty acids (SCFAs) analysis. The SCFA concentration was determined according to our previous study.¹⁸ Briefly, colonic contents (50 mg) were extracted ultrasonically with 1 mL of ice-cold saline for 5 min and subsequently centrifuged for 5 min (12 000g, 4 °C). The supernatant was gathered and extracted with metaphosphoric acid (9:1 v/v) at 25% (w/v). Supernatants were collected after centrifugation (12 000g, 5 min, 4 °C) of the extraction. The HP-FFAP capillary column (Agilent, Folsom, CA, USA) was equipped with a SHIMADZU GC2030-QP2020 NX gas chromatography-mass spectrometer (Kyoto, Japan). An Agilent capillary column HP-FFAP coupled to a gas chromatography-mass spectrometer SHIMADZU GC2030-QP2020 NX (Kyoto, Japan) was used for further testing. Flow rates of the front inlet purge

Table 1 The composition of the diet

Component	LG	CPD	UCPD
Casein/g	70	0	0
L-Cystine/g	3	3	3
Ultrasound chickpea protein/g	—	—	230.422
Chickpea protein/g	—	230.279	—
Corn starch/g	527.5	367.221	367.078
Maltodextrin 10/g	132	132	132
Sucrose/g	100	100	100
Cellulose, BW200/g	50	50	50
Lard/g	70	70	70
Vitamin mix V10037/g	10	10	10
Mineral mix S10022G/g	35	35	35
Choline bitartrate/g	2.5	2.5	2.5
FD&C red dye #40/g	—	0	0.025
FD&C yellow dye #5	—	0	0
FD&C blue dye #1	—	0.05	0.025
Energy density/kcal g ⁻¹	4.00	4.00	3.99
Macronutrient content/g	952.5	952.4	952.5
Micronutrient content/g	47.5	47.5	47.5
Ingredient amount/g	0	0.05	0.05
Total/g	1000	1000	1000
Protein (%)	7.30	23.32	23.34
Carbohydrate (%)	80.95	64.92	64.91
Fat (%)	7.00	7.00	7.00

The abbreviations are as follows: 7% protein group (LG), chickpea protein diet (CPD), ultrasound chickpea protein diet (UCPD).



and gas were 3 mL min^{-1} and 1 mL min^{-1} , respectively. The temperature at the start was $80 \text{ }^\circ\text{C}$ and finally, the temperature was $240 \text{ }^\circ\text{C}$. In the electronic impact mode, the energy was -70 eV . The scan/SIM mode was used for acquiring mass spectrometry data.

2.4.3. 16S rRNA gene sequences. Colonic samples were collected for extraction using An E.N.Z.A.® Stool DNA isolation kit according to the protocol of the manufacturer (primer 5'-ACTCCTACGGGAGGCAGCA-3' and reverse primer 5'-GGACTACHVGGGTWTCTAAT-3' targeting the V3-V4 hypervariable region). Samples of the microbial genomic DNA and raw data were sequenced and analyzed on the library of the Illumina HiSeq 2500 (Illumina, San Diego, California, USA) instrument. OTUs were clustered based on 97% similarity according to the Greengenes database (V.13.8). At the phylum, order, and genus levels, relative abundances were calculated. An analysis of the rarefaction was conducted using the alpha diversity index (Shannon index).

2.5. Statistical analysis

Analysis of the obtained data was conducted using SPSS version 20 (SPSS, Chicago, IL, USA). The data were expressed as mean \pm standard deviation (SD). Figures were painted by GraphPad Prism 9. Statistical significance among the groups was carried out by one-way ANOVA followed by the Tukey post-test. The correlation analysis was identified by Spearman's correlation. A p -value below 0.05 was considered significant.

3. Results and discussion

3.1. Particle size and ζ -potential

The particle size is an important index that affected solubility, emulsification, and foamability.⁹ It sharply decreased by 205.18% in UCP compared to CP (Fig. 1a), which largely decreased than that compared in a previous study of chickpea protein isolates after HIU because the treatment time in the present study was 30 min, while 20 min was implemented in Wang's study.¹³ The HIU accelerates the collision of proteins by generating cavitation and shear force, thus proteins became smaller when more time was implemented on them.¹⁹ In addition, the energy produced by the HIU broke the hydrogen bonding between proteins and simultaneously decreased particle size.²⁰ The CLSM and TEM results also showed a significant change in the particle size between CP and UCP, which evidenced the change in the particle size (Fig. 1b and f).

ζ -potential, is an important factor that influences protein aggregation and reflects the ionization degree of protein.²¹ After the HIU treatment, UCP showed significantly higher absolute ζ -potential values compared to CP (Fig. 1c). Zhang *et al.* (2022) also reported similar results that HIU treatment increased the ζ -potential of the pea protein under different ultrasound power (200–600 W), and as the ultrasound power increased, the ζ -potential values grew (synergistic modification of pea protein structure using high-intensity ultrasound and pH-shifting technology to improve solubility and emulsification). The increase in ζ -potential may be due to the exposure of the internal polar groups, thus can enhance electrostatic repulsions and solubility.

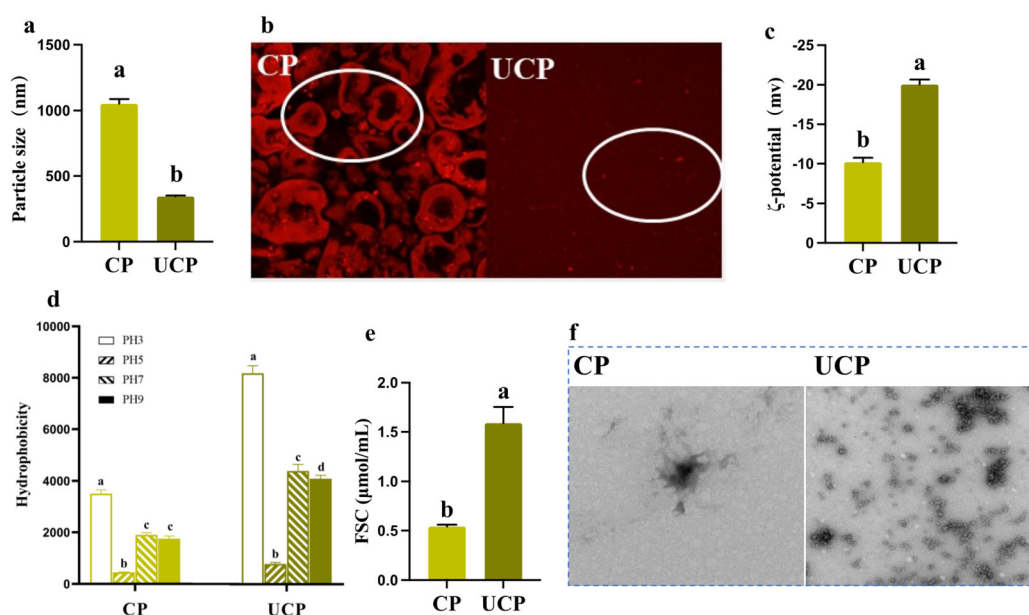


Fig. 1 The physicochemical properties of CP and UCP. (a) The particle size of CP and UCP. (b) The CP and UCP were observed by a confocal laser scanning microscope. (c) The ζ -potential of CP and UCP. (d) The hydrophobicity at different pHs (pH 3, 5, 7, and 9) of CP and UCP. (e) The FSC of CP and UCP. (f) The TEM images of CP and UCP. Data were presented as mean \pm SD. CP means chickpea protein; UCP means ultrasound chickpea protein; FSC means free sulphhydryl content. The different letters on the bar mean the statistical difference between groups ($p < 0.05$).



3.2. Hydrophobicity and FSC

Hydrophilic and hydrophobic groups are important indices in evaluating the change of the conformation and surface charge in legume protein.⁵ In this study, the surface hydrophobicity of CP was the lowest at pH 5.0, but increased at pH 3.0, 7.0, and 9.0. The hydrophobicity in UCP was statistically increased by 134.29%, 175.56%, 131.57%, and 134.28% compared to CP at different pHs, black soybean protein treated at 150 W for 24 min showed the same trend.⁸ While in this study, the ultrasound time was 30 min (150 W), thus the hydrophobicity in UCP was upregulated higher than in black soybean bean protein (Fig. 1d). The HIU caused the exposure of more hydrophobic groups that were buried inside before treatment, which then increased the surface hydrophobicity.⁵ Higher hydrophobicity was uncovered at pH 3.0 than at 7.0 and 9.0 may be because the dissociation of protein subunits at pH 3.0 exposed more hydrophobic regions.²² In addition, the change of hydrophobicity meant that the alteration happened between hydrophilic and hydrophobic groups, and this was one of the most important factors affecting the ζ -potential.¹⁰

Apart from the increase in hydrophobicity, ultrasound treatment also induced the gradual exposure of free sulfhydryl groups initially buried in the protein to the protein surface. FSC plays a fundamental role in determining the functional properties of protein.⁵ The FSC was increased by 193.36% in UCP compared to CP (Fig. 1e), which was inconsistent with several published literature.^{13,23,24} There are two main reasons that can result in the increased FSC. The strong ultrasonic shear waves could unfold the protein structure, leading to the exposure of the internal -SH and converting it into FSC. Meanwhile, because of the acoustic cavitation effect, particle size decreases along with intermolecular S-S breakdown, which together led to the increase of FSC in our study.^{25–27}

The change in the particle size reflected that the interactions in protein aggregates were broken, thus showing the smaller particle size in UCP. In addition, the energy force input by HIU caused more hydrophobic groups and free sulfhydryl exposure, then the ζ -potential, hydrophobicity, and FSC increased statistically in UCP compared to CP. Moreover, these changes were also related to functional properties (solubility, emulsifying, and foamability), which were consistent with the previous study. Therefore, these functional properties are measured and discussed as follows.

3.3. Solubility

Solubility is a fundamental protein function closely associated with particle size and ζ -potential.⁵ As shown in Fig. 2a, the solubility of CP and UCP at pH 3.0, 5.0, 7.0, and 9.0. It can be found that CP and UCP showed a typical “U-shape” distribution of the solubility–pH profile, with the lowest values near the isoelectric point (pH 5.0), and a significant increase as the pH deviated from 5.0. Similar pH-dependent profiles of CP have been reported by Ghribi *et al.*, (2015).²⁸ The solubility was statistically increased by 25.34%, 36.27%, 12.57%, and 18.94% in UCP compared to CP at different pHs. UCP showed higher

solubility compared to that in a previous study in chickpea protein isolates because of the smaller particle size and higher ζ -potential in this study than their results.¹³ Even though the increased hydrophobicity could result in decreased solubility in a general way, in our study, the particle size of the protein sharply decreased and ζ -potential enhanced the result of mechanical force generated by HIU at the same time, increasing the surface contact area between protein particles and water, which can together result in an increase in the water solubility.¹⁹ The ultrasonication treatment can improve functional characteristics related to the increased solubility of proteins, thus solubility is one of the most important indices of proteins used in the food industry.⁷

3.4. Emulsion and foaming capability

The EAI is an important index in food processing and production. Both EAI and ESI were improved in UCP. The EAI increased by 62.96%, 54.29%, 47.85%, and 60.33%, respectively at different pHs in UCP compared to CP, and the ESI was simultaneously upregulated by 29.17%, 31.09%, 31.70%, and 38.71% at different pHs in UCP (Fig. 2b and c). The increase of EAI and ESI was associated with the rising of hydrophobicity and the decrease of the surface charge in UCP due to the adsorption rate influenced by the surface hydrophobicity and net electric repulsion, thus the increase of hydrophobicity and ζ -potential contributed to the improvement of EAI and ESI.²⁰ A previous report on chickpea protein isolates after ultrasonication showed lower EAI and ESI compared with UCP because their results of physicochemical properties (particle size, ζ -potential, hydrophobicity, and FSC) were not as good as UCP.¹³ In addition, the better performance of solubility in UCP also contributed to enhancing EAI and ESI.¹⁹ The EAI and ESI are important factors in food production, the higher EAI and ESI results in a better sensory experience for the customer.

Foam capacities (FA and FS) are indispensable quality indices in some special food production (cake, ice cream, and candy).⁵ The foam was generated when the protein solution was homogenized at a high speed, bringing more air into the solution. As shown in Fig. 2d, the FA was statistically improved by 105.35%, 164.89%, 132.96%, and 196.37%. CP showed the lowest foaming properties at pH 5.0 due to their lower protein solubility and hydrophobicity. As shown in Fig. 2e, compared to CP, UCP maintained the same trend at different pHs, which is consistent with a previous study that reported the improvement of the particle size and hydrophobicity encouraged better performance in FA.¹⁰ The alleviation of FA induced by ultrasonication was associated with the decrease of particle size and the increase of hydrophobicity because it gives more opportunity to protein when contacting with air, and subsequently alleviated FA.²⁹

3.5. SDS-PAGE and FTIR

To explain in-depth the mechanism of the functional properties change between CP and UCP, structural properties were studied, including SDS-PAGE and FTIR. There are several types



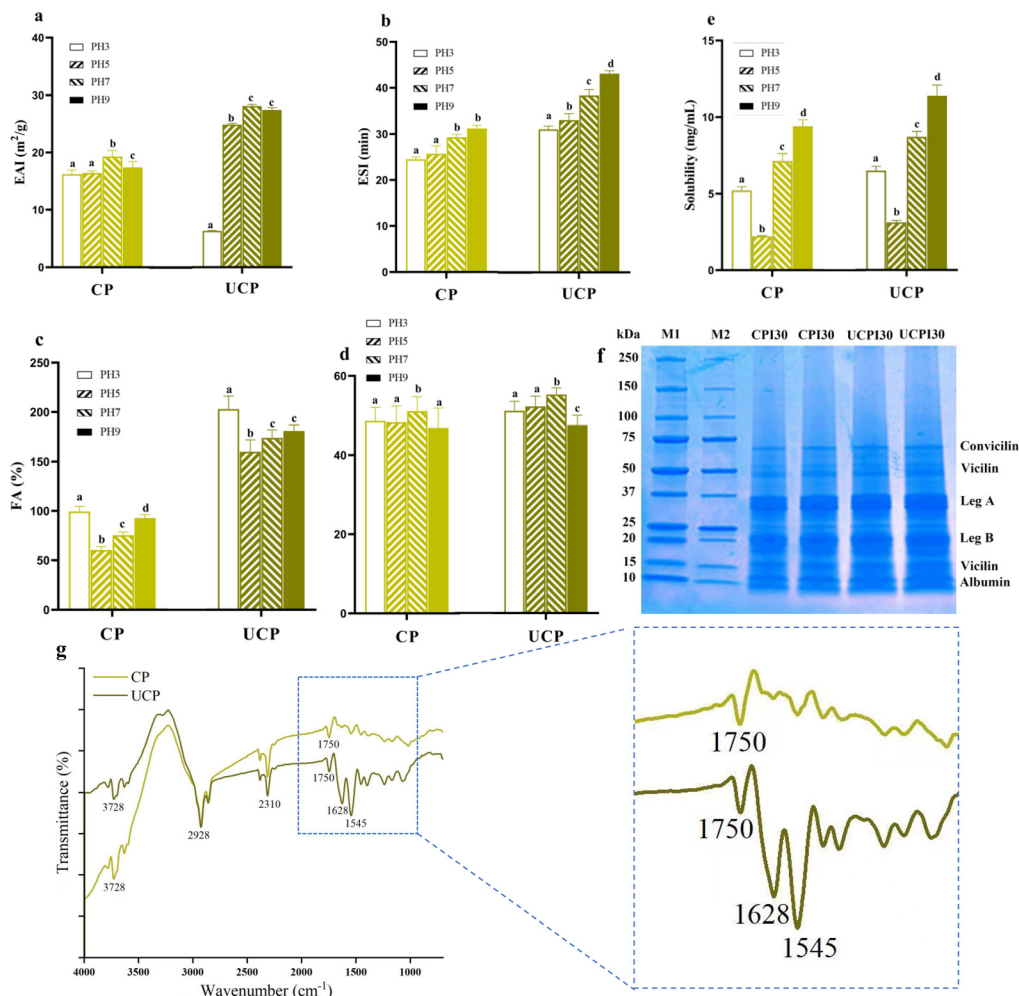


Fig. 2 The functional properties at different pHs (pH 3, 5, 7, and 9) and structure properties of CP and UCP. (a) The solubility; (b) the EAI; (c) the ESI; (d) the FA; (e) the FS; (f) the SDS-PAGE (g) FTIR. Data were presented as mean \pm SD. CP means chickpea protein; UCP means ultrasound chickpea protein; EAI means emulsifying activity; ESI means emulsifying stability; FA means foaming ability; FS means foaming stability. SDS-PAGE means sodium dodecyl-sulfate polyacrylamide gel electrophoresis; FTIR means Fourier transform infrared. The different letters on the bar mean the statistical difference between groups ($p < 0.05$).

of proteins in chickpeas, primarily globulins (11S legumins, 7S vicilins, and 8S convicilins) and albumins (2S). An acidic polypeptide (leg A) and a basic polypeptide (leg B) make up the 11S legumin. According to our results, CP and UCP showed no significant differences in bands, indicating that HIU treatment did not affect the types and molecular weight of protein subunits. Yuntao Wang *et al.* (2020)³⁰ also reported similar results that HIU treatment (300 W for 5, 10, and 20 min) did not induce the degradation or crosslinking of chickpea protein. While this result was different from that of HIU-treated seed isolate protein, which found a molecular weight change after different HIU powers (200 W, 400 W, and 600 W).³¹ The reason for the discrepancy might be related to the primary structure of the protein and the treatment conditions of HIU, such as treatment time and power level.

Furthermore, FTIR spectra (ranging between 400 and 4000 cm^{-1}) were collected to observe the secondary structure

of CP and UCP. A considerable change was detected in amide I ($\sim 1600 \text{ cm}^{-1}$) and amide II ($\sim 1500 \text{ cm}^{-1}$). The amides I and II reflect the C–O stretching vibrations and CO–NH stretching, respectively, which are strongly influenced by the secondary structure of the protein, including aggregation, folding, and unfolding.³² Our results showed that HIU significantly altered the secondary structure of the protein, which is consistent with many published works of literature regarding the HIU treatment on protein. By breaking hydrogen bonds between proteins and increasing protein flexibility caused by the cavitation effect, HIU treatment alters secondary structures in proteins.³³

By cavitating and micro-streaming, the HIU modified the secondary structure of chickpea protein, exposing hydrophobic amino acid residues, resulting in an increase in hydrophobicity and zeta potential, thus the emulsion properties are enhanced. Meanwhile, the particle size sharply decreased,



leading to improved solubility and foaming ability. Furthermore, these surface amino acids enhanced the potential of CP applications in alleviating malnutrition. A previous study reported that chickpea flour showed positive performance in improving growth in undernourished children by regulating gut microbiota.

3.6. Body weight, tail length, IGF-1, and ACE 2

The undernourished rat model was successfully constructed by the administration of 7% casein for 3 weeks with statistical body weight loss ($43.58\% \pm 2.39$) compared to normal rats. Two different chickpea protein diets alleviated body weight and tail length at different levels (Fig. 3a and b). Body weight and tail length directly reflect the improvement in malnutrition.³⁴ After 6 weeks of treatment, the body weight in CPD and UCPD increased by 53.76% and 72.16%, respectively, compared with that in LG (Fig. 3a), which was similar to the report by Gehrig *et al.* who observed that diets with chickpea flour improved body weight loss in children with moderate malnutrition.³⁵ Similarly, the tail lengths in CPD and UCPD increased by 9.61% and 11.83% compared to that in LG (Fig. 3b). In this study, CP and UCP were added to supplementary diets and showed good performance in alleviating malnutrition in rats, while UCPD performed better in alleviating growth, which showed an increase by 11.97% and 2.03% in

body weight and tail length, respectively, compared to CPD (Fig. 3a and b). With the improvement of solubility and the exposure of amino acids, which are primarily buried in hydrophobic regions by ultrasonication, the digestibility of legume protein simultaneously alleviated.³⁶ The digestibility of proteins is directly related to hosting health because amino acids from the breakdown of dietary protein would be absorbed in the small intestine and influence the metabolism of the host.³⁷ Therefore, the better physicochemical (particle size, ζ -potential, hydrophobicity, and FSC), functional properties (solubility, EAI, and ESI), and digestibility in CP after ultrasonication may explain why UCPD performed better than CPD in alleviating malnutrition.

As a key factor in growth, IGF-1 is produced by the growth hormone secreted by the pituitary gland. Recent studies have demonstrated that IGF-1 plays a critical role in the proliferation, differentiation, division, and survival of somatic cells.³⁸ The level of IGF-1 statistically decreased in LG by 26.17% and 36.82% compared with CPD and UCPD, respectively, which is the same as that in a previous report that showed that plant-protein increased the activity of the IGF-1 system (Fig. 3c).³⁹ A study reported that weight gain was positively correlated with IGF-1.⁴⁰ Therefore, the insufficient secretion of IGF-1 causes growth deficiency. Also, ACE 2 decreased significantly in LG, while it was sharply reduced by 28.68% and 48.85% compared to CPD and UCPD, respectively, after the supplementary diet (Fig. 3d). A previous study proved that the production of IGF-1 was associated with the microbes in the gut and the lack of ACE 2 implemented the impact of dietary amino acid homeostasis and gut microbial ecology.⁴¹ In addition, gut microbiota also placed an impact on the production of ACE 2, which could improve intestinal integrity.⁴²

3.7. Analysis of SCFAs

Playing a crucial role in host health, SCFAs were significantly decreased in undernourished mice (Wei, *et al.*, 2021). These results showed that the total SCFA concentration and the components of SCFAs were all strikingly impacted by a three-week inefficient protein diet. The CPD and UCPD had the highest content in total SCFAs, which were upregulated by 90.12% and 157.89%, respectively, than in LG (Fig. 4a). Rats' supplementary insufficient protein diet had the lowest level of SCFAs, which was similar to a previous study that showed sharply decreased SCFAs in undernourished children (Fig. 4a).³⁵ In addition, SCFAs still changed when dietary fiber was removed by washing the undigested residue with ethanol and acetone, indicating that protein, as the fermentation subtracts gut microbiota, caused SCFAs to rise.⁴³ Butyrate and propionate have been suggested to have unique effects on host energy metabolism and immune regulation.⁴⁴ Therefore, a considerable decrease in butyrate and propionate in LG revealed the damage to the health of the host in undernourished rats. Comfortingly, following supplementary food improved the production of butyrate, thus improving the host's health. Based on our knowledge, limited studies have explained and com-

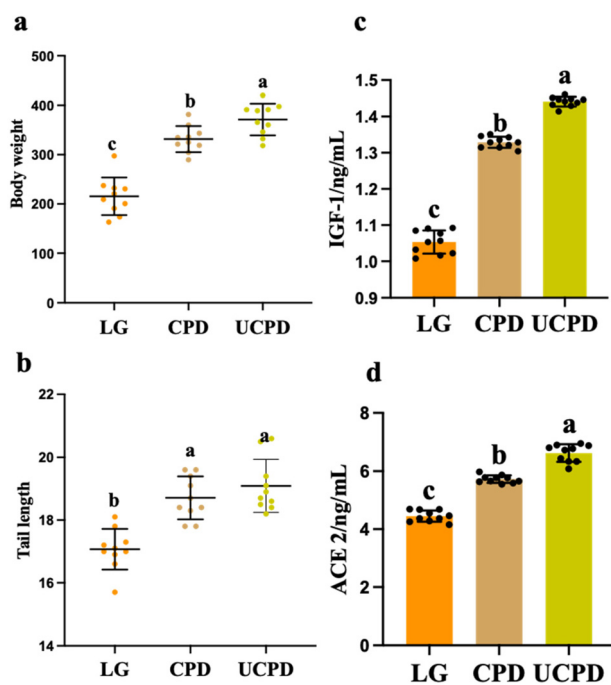


Fig. 3 The growth indexes of undernourished rats after supplementary CPD and UCPD. (a) The body weight among groups. (b) The tail length among groups. (c) The IGF-1 among groups. (d) The ACE 2 among groups. Data were presented as mean \pm SD. CPD means chickpea protein diet; UCPD means ultrasound chickpea protein diet; IGF-1 means insulin-like growth factor-1; ACE 2 means angiotensin-converting enzyme 2. The different letters on the bar mean the statistical difference between groups ($p < 0.05$).



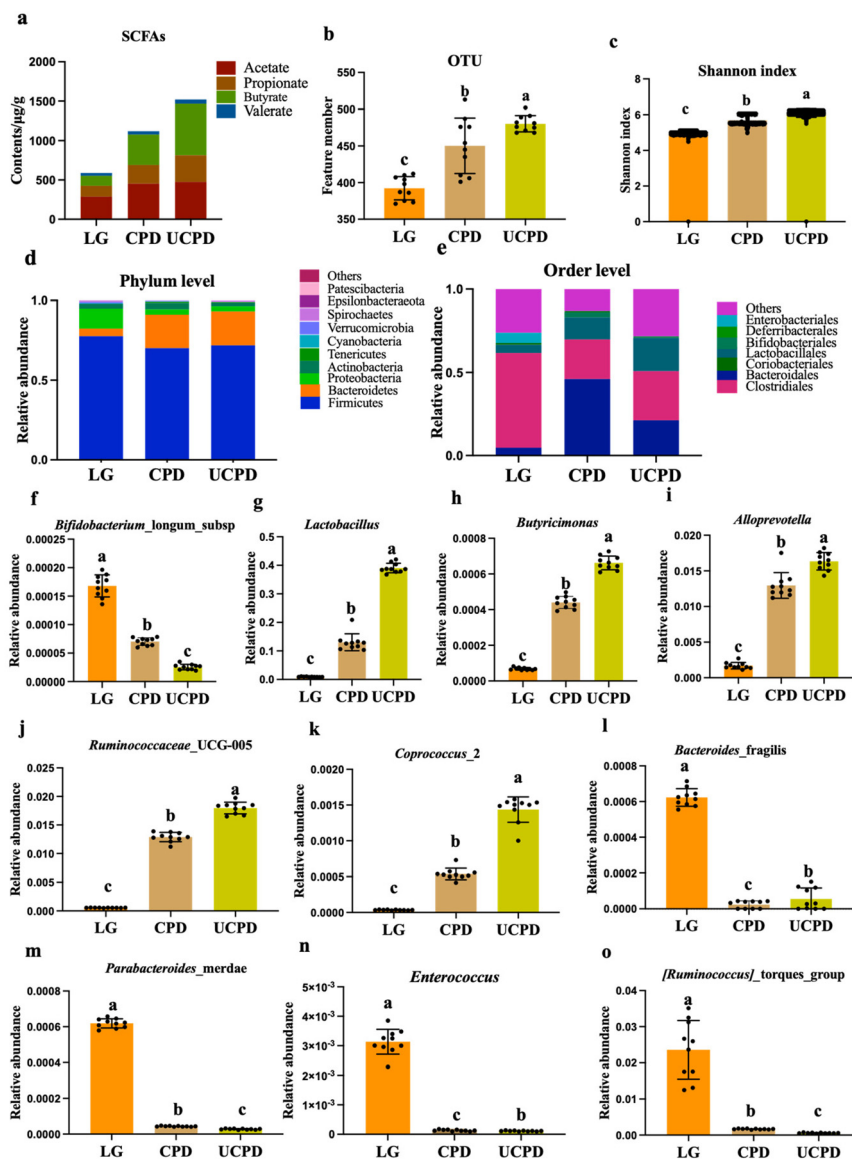


Fig. 4 The change of gut compositions among groups. (a) The SCFAs among groups. (b) The OTU among groups. (c) The Shannon index among groups. (d) The gut microbiota at the phylum level among groups. (e) The gut microbiota at the order level. (f) The relative content of *Bifidobacterium_longum_subsp.* among groups. (g) The relative content of *Lactobacillus* among groups. (h) The relative content of *Butyricimonas* among groups. (i) The relative content of *Alloprevotella* among groups. (j) The relative content of *Ruminococcaceae_UCG-005* among groups. (k) The relative content of *Coprococcus_2* among groups. (l) The relative content of *Bacteroides_fragilis* among groups. (m) The relative content of *Parabacteroides merdae* among groups. (n) The relative content of *Enterococcus* among groups. (o) The relative content of *Ruminococcus torques* among groups. Data were presented as mean \pm SD. CPD means chickpea protein diet; UCPD means ultrasound chickpea protein diet; SCFA means short-chain fatty acid. The different letters on the bar mean the statistical difference between groups ($p < 0.05$).

pared the effect of ultrasonic leguminous protein on gut microbiota and metabolites.

3.8. Gut microbiota composition in rats

Diet supplementary chickpea flour statistically improved gut microbiota in gnotobiotic mice, which received the gut community contributed by children with post-server acute malnutrition and moderate acute malnutrition.³⁵ Therefore, 16S rRNA sequencing was used to measure the change in gut microbiota among the groups. Nevertheless, OTU was restored

by 14.78% and 22.43% in CPD and UCPD, respectively, compared with LG (Fig. 4b). The Shannon index of alpha diversity was used to measure species diversity and was determined by the species abundance and species uniformity in the sample community, which decreased by 12.32% and 18.21%, respectively, in LG compared to that in CPD and UCPD (Fig. 4c). The change in OTU and Shannon index in LG was evidenced in a previous study, which reported that undernutrition influenced gut microbiota in its structure and diversity.⁴⁵ More importantly, UCPD showed better improvement than CPD in restor-



ing gut microbiota. A limited study has reported the relationship between UCP and gut microbiota. But UCP performed better in solubility, emulsifying, and foamability, which were mentioned above. Although a previous result claimed that ultrasound processing failed to change the secondary structure of chickpea protein, the unfolding of the protein structure-endowed proteins with some unique properties.⁴⁶ Gut microbiota in undernutrition weaning rats may not efficiently apply macromolecular protein because of the damage to gut barrier and metabolism, thus UCP performed better in alleviating the richness and diversity of gut microbiota. Back to the phylum level, it was clear that *Firmicutes*, *Bacteroidetes*, and *Proteobacteria* were predominant in each group, but the ratio of these bacteria changed significantly in different groups (Fig. 4d). In the CPD and UCPD, *Bacteroidetes* statistically increased by 343.05% and 346.25%, respectively, compared to that in LG. But *Firmicutes* and *Proteobacteria* were decreased in CPD and UCPD (Fig. 4d). At the phylum level, it was difficult to demonstrate the change of varied diets. Therefore, the order level is shown in Fig. 4e. *Clostridiales* and *Bacteroidales* accounted for over 50%, and *Lactobacillales* showed statistical changes among groups (Fig. 4e). Gut was modulated to a healthier status, which means reducing potentially pathogenic bacteria, for instance, *Bacteroides fragilis*, *Parabacteroides merdae*, *Enterococcus*, and *Ruminococcus torques*, which decreased gut barrier integrity or induced gut inflammation, while increasing beneficial bacteria such as *Lactobacillales*, *Butyricimonas*, *Bifidobacterium longum* subsp., *Alloprevotella*, *Coprococcus_2*, and *Ruminococcaceae_UCG-005*.^{47–50} Therefore, ten bacteria were chosen to compare the relative abundance at the genus level (Fig. 4f–o).

Bifidobacterium longum subsp. decreased by 58.23% and 84.78% in CPD and UCPD, respectively, compared with LG (Fig. 4f). Obviously, UCPD decreased more than CPD. The *Bifidobacterium longum* subsp. was reported using the toll-like receptor 4 (TLR-4) in immature enterocytes for anti-inflammation by attenuating interleukin-6 (IL-6) induction in response.⁵¹ Therefore, the relative abundance of higher *Bifidobacterium longum* subsp. in LG reflected the inflammation induced by malnutrition, which was reported in a previous study that malnutrition was related to intestinal inflammation among undernourished children. The *Lactobacillus* significantly increased by 12.89-fold and 40.65-fold in CPD and UCPD compared to that in LG, respectively, which play a unique role in the proteolytic system of gut bacteria (Fig. 4g).⁵² *Butyricimonas* and *Alloprevotella* are considered as relating to the production of SCFAs^{53,54} which were alleviated by 545.86%, 661.74%, and 861.21%, 870.88% in CPD and UCPD, respectively, than in LG (Fig. 4h and i). Moreover, the dominant abundance genera of the healthy gut (*Ruminococcaceae_UCG-005* and *Coprococcus_2*) were notably restored in CPD and UCPD compared to that in LG, respectively (Fig. 4j and k).⁴⁹ For alleviating malnutrition, modifying the abundance of harmful bacteria in the gut is important. Enterotoxigenic *Bacteroides fragilis* was claimed to link with undernutrition because it perturbs gut barrier function.⁵⁵ In

this study, the same phenomenon was observed in LG in which the relative content of *Bacteroides fragilis* was higher than that in CPD and UCPD, while that in UCPD was lower than that in CPD (Fig. 4l). In addition, *Parabacteroides merdae*, *Enterococcus* and *Ruminococcus torques* were statistically decreased in CPD and UCPD indicating that the damaged gut induced by malnutrition was transformed to healthier one (Fig. 4m–o).

3.9. Integrated multi-OMINCS

Having obtained different omics substances that were influenced by supplementary diets in undernourished rats, the next step was to study the interplay among the body weight, tail length, and gut microbiota components (Fig. 5).

Before multi-OMICS analysis, ten bacteria in the gut were selected based on studies conducted OMICS analysis with growth indicators and SCFAs. As shown in Fig. 5, the beneficial bacteria, such as *Lactobacillales*, *Butyricimonas*, *Alloprevotella*, *Coprococcus_2*, and *Ruminococcaceae_UCG-005* were positively related to body weight and tail length, while other bacteria were negatively associated with growth indicators.

The effect of chickpea flour on improving malnutrition was reported in a previous study.³⁵ In this study, CP showed the same improvement, furthermore, UCP showed a better effect on modulating undernutrition. It is widely known that stunted growth is a notable feature of malnutrition. Recent studies have revealed the relationship between malnutrition and gut microbiota and subsequently produced microbiota-directed food to alleviate undernutrition.⁵⁶ The change in gut microbiota was mainly from the imbalance of beneficial and harmful bacteria at different ages. In the present study, beneficial bacteria (*Lactobacillales*, *Butyricimonas*, *Alloprevotella*, *Coprococcus_2*, and *Ruminococcaceae_UCG-005*) were alleviated after supplementary CPD and UCPD and showed growth recov-

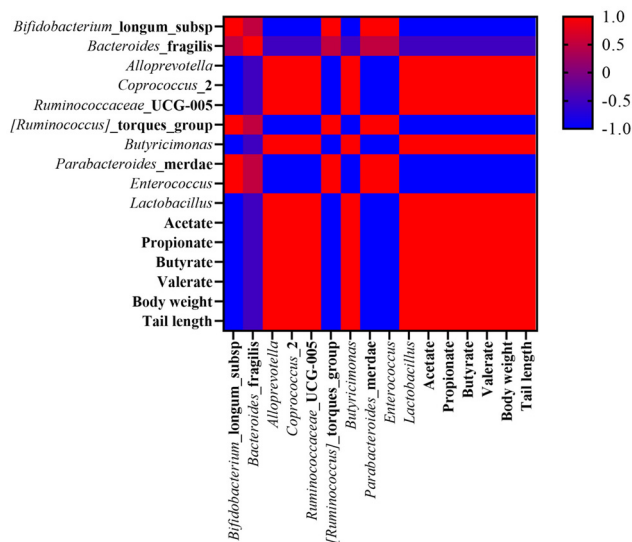


Fig. 5 The correlation between growth indexes and gut compositions among groups.



ery. Diarrhea and intestinal inflammation are common in malnourished children due to a damaged gut.⁵⁷ A damaged gut environment is difficult to digest and absorb nutrition from diet and subsequently caused undernutrition. In this study, supplementary CPD and UCPD reshaped the gut microbiota system, and UCP showed better physicochemical properties supported in alleviating undernourished rats better than CP. SCFAs played as important regulators in intestinal immunity with anti-inflammatory properties and provided energy to enterocytes and modulate metabolism.⁵⁷

4. Conclusions

After HIU treatment (150 W, 30 min), the physicochemical and structural properties of CP changed, resulting in an increase in solubility, emulsion, and foaming ability, thus allowing the modified UCP to be used as surfactants, bioactive compounds, and other additives for food or pharmaceutical products. Furthermore, rats supplemented with CPD and UCPD positively upregulated growth *via* the gut microbiota. In addition, UCPD performed better than CPD in improving malnutrition. The change in SCFA production and gut microbiota revealed the internal mechanism of CP and UCP alleviating malnutrition. However, this study also has limitations. In the animal experiments, another control with 23.32% casein should be added, which can be better than the chickpea treatment at the same protein content level. Overall, this research will encourage and provide new insights into the applications of CP and UCP.

Conflicts of interest

There are no conflicts to declare.

Acknowledgements

This work was supported by the Special National Key Research and Development Plan (2021YFD1600100), the Opening Project of the Key Laboratory of Coarse Cereal Processing of the Ministry of Agriculture and Rural Affairs, and Sichuan Engineering and Technology Research Center of Coarse Cereal Industrialization, Chengdu University (no. 2022-CC008), the Science and Technology Research Projects of Chongqing Education Commission (grant nos. KJQN202102705), Key Laboratory of Grain Crop Genetic Resources Evaluation and Utilization, China Agriculture Research System of MOF and MARA (CARS-08-G21) (Food Legumes).

References

- H. H. Fore, Q. Dongyu, D. M. Beasley and T. A. Ghebreyesus, Child malnutrition and COVID-19: the time to act is now, *Lancet*, 2020, **396**, 517–518.
- K. A. A. Martinez and E. G. Mejia, Comparison of five chickpea varieties, optimization of hydrolysates production and evaluation of biomarkers for type 2 diabetes, *Food Res. Int.*, 2021, **147**, 110572.
- A. Matemu, S. Nakamura and S. Katayama, Health Benefits of Antioxidative Peptides Derived from Legume Proteins with a High Amino Acid Score, *Antioxidants*, 2021, **10**, 316.
- Y. J. Xu, M. Dong, C. B. Tang, M. Y. Han, X. L. Xu and G. H. Zhou, Glycation-induced structural modification of myofibrillar protein and its relation to emulsifying properties, *LWT – Food Sci. Technol.*, 2020, **117**, 108664.
- S. M. T. Gharibzadeh and B. Smith, The functional modification of legume proteins by ultrasonication: A review, *Trends Food Sci. Technol.*, 2020, **98**, 107–116.
- T. Zheng, X. H. Li, A. Taha, Y. Wei, T. Hu, P. B. Fatamorgana, Z. Zhang, F. X. Liu, X. Y. Xu, S. Y. Pan and H. Hu, Effect of high intensity ultrasound on the structure and physicochemical properties of soy protein isolates produced by different denaturation methods, *Food Hydrocolloids*, 2019, **97**, 105216.
- S. S. Jiang, J. Z. Ding, J. Andrade, T. M. Rababah, A. Almajwal, M. M. Abulmeaty and H. Feng, Modifying the physicochemical properties of pea protein by pH-shifting and ultrasound combined treatments, *Ultrason. Sonochem.*, 2017, **38**, 835–842.
- L. Z. Jiang, J. Wang, Y. Li, Z. J. Wang, J. Liang, R. Wang, Y. Chen, W. J. Ma, B. K. Qi and M. Zhang, Effects of ultrasound on the structure and physical properties of black bean protein isolates, *Food Res. Int.*, 2014, **62**, 595–601.
- J. O'Sullivan, B. Murray, C. Flynn and I. Norton, The effect of ultrasound treatment on the structural, physical and emulsifying properties of animal and vegetable proteins, *Food Hydrocolloids*, 2016, **53**, 141–154.
- A. Martinez-Velasco, C. Lobato-Calleros, B. E. Hernandez-Rodriguez, A. Roman-Guerrero, J. Alvarez-Ramirez and E. J. Vernon-Carter, High intensity ultrasound treatment of faba bean (*Vicia faba* L.) protein: Effect on surface properties, foaming ability and structural changes, *Ultrason. Sonochem.*, 2018, **44**, 97–105.
- J. Quintero-Quiroz, A. Celis-Torres, G. Ciro-Gomez, J. Torres, L. Corrales-Garcia and J. Rojas, Physicochemical properties and functional characteristics of ultrasound-assisted legume-protein isolates: a comparative study, *J. Food Sci. Technol.*, 2021, 1–12.
- S. H. Peighambaroust, A. J. van der Goot, R. J. Hamer and R. M. Boom, Effect of simple shear on the physical properties of glutenin macro polymer (GMP), *J. Cereal Sci.*, 2005, **42**, 59–68.
- Y. T. Wang, Y. J. Wang, K. Li, Y. H. Bai, B. Li and W. Xu, Effect of high intensity ultrasound on physicochemical, interfacial and gel properties of chickpea protein isolate, *LWT – Food Sci. Technol.*, 2020, **129**, 109563.
- H. Hu, J. H. Wu, E. C. Y. Li-Chan, L. Zhu, F. Zhang, X. Y. Xu, G. Fan, L. F. Wang, X. J. Huang and S. Y. Pan, Effects of ultrasound on structural and physical properties



- of soy protein isolate (SPI) dispersions, *Food Hydrocolloids*, 2013, **30**, 647–655.
- 15 N. Vakondios, E. E. Koukouraki and E. Diamadopoulos, Effluent organic matter (EfOM) characterization by simultaneous measurement of proteins and humic matter, *Water Res.*, 2014, **63**, 62–70.
 - 16 D. Dong and B. Cui, Fabrication, characterization and emulsifying properties of potato starch/soy protein complexes in acidic conditions, *Food Hydrocolloids*, 2021, **115**, 106600.
 - 17 E. M. Brown, M. Wlodarska, B. P. Willing, P. Vonaesch, J. Han, L. A. Reynolds, M. C. Arrieta, M. Uhrig, R. Scholz, O. Partida, C. H. Borchers, P. J. Sansonetti and B. B. Finlay, Diet and specific microbial exposure trigger features of environmental enteropathy in a novel murine model, *Nat. Commun.*, 2015, **6**, 1–16.
 - 18 Z. Shi, Y. Zhu, C. Teng, Y. Yao, G. Ren and A. Richel, Anti-obesity effects of alpha-amylase inhibitor enriched-extract from white common beans (*Phaseolus vulgaris* L.) associated with the modulation of gut microbiota composition in high-fat diet-induced obese rats, *Food Funct.*, 2020, **11**, 1624–1634.
 - 19 Z. B. Zhu, W. D. Zhu, J. H. Yi, N. Liu, Y. G. Cao, J. L. Lu, E. A. Decker and D. J. McClements, Effects of sonication on the physicochemical and functional properties of walnut protein isolate, *Food Res. Int.*, 2018, **106**, 853–861.
 - 20 W. C. Ma, J. M. Wang, X. B. Xu, L. Qin, C. Wu and M. Du, Ultrasound treatment improved the physicochemical characteristics of cod protein and enhanced the stability of oil-in-water emulsion, *Food Res. Int.*, 2019, **121**, 247–256.
 - 21 Y. X. Chen, L. Sheng, M. Gouda and M. H. Ma, Impact of ultrasound treatment on the foaming and physicochemical properties of egg white during cold storage, *LWT – Food Sci. Technol.*, 2019, **113**, 108303.
 - 22 C. Chang, S. Tu, S. Ghosh and M. Nickerson, Effect of pH on the inter-relationships between the physicochemical, interfacial and emulsifying properties for pea, soy, lentil and canola protein isolates, *Food Res. Int.*, 2015, **77**, 360–367.
 - 23 T. Zheng, X. Li, A. Taha, Y. Wei, T. Hu, P. B. Fatamorgana, Z. Zhang, F. Liu, X. Xu and S. Pan, Effect of high intensity ultrasound on the structure and physicochemical properties of soy protein isolates produced by different denaturation methods, *Food Hydrocolloids*, 2019, **97**, 105216.
 - 24 R. Mozafarpour, A. Koocheki and T. Nicolai, Modification of grass pea protein isolate (*Lathyrus sativus* L.) using high intensity ultrasound treatment: Structure and functional properties, *Food Res. Int.*, 2022, **158**, 111520.
 - 25 H. Hu, J. Wu, E. C. Li-Chan, L. Zhu, F. Zhang, X. Xu, G. Fan, L. Wang, X. Huang and S. Pan, Effects of ultrasound on structural and physical properties of soy protein isolate (SPI) dispersions, *Food Hydrocolloids*, 2013, **30**, 647–655.
 - 26 H. Huang, K.-C. Kwok and H.-H. Liang, Inhibitory activity and conformation changes of soybean trypsin inhibitors induced by ultrasound, *Ultrason. Sonochem.*, 2008, **15**, 724–730.
 - 27 T. Xiong, W. Xiong, M. Ge, J. Xia, B. Li and Y. Chen, Effect of high intensity ultrasound on structure and foaming properties of pea protein isolate, *Food Res. Int.*, 2018, **109**, 260–267.
 - 28 A. M. Ghribi, I. M. Gafsi, C. Blecker, S. Danthine, H. Attia and S. Besbes, Effect of drying methods on physico-chemical and functional properties of chickpea protein concentrates, *J. Food Eng.*, 2015, **165**, 179–188.
 - 29 M. A. Malik, H. K. Sharma and C. S. Saini, High intensity ultrasound treatment of protein isolate extracted from dephenolized sunflower meal: Effect on physicochemical and functional properties, *Ultrason. Sonochem.*, 2017, **39**, 511–519.
 - 30 Y. Wang, Y. Wang, K. Li, Y. Bai, B. Li and W. Xu, Effect of high intensity ultrasound on physicochemical, interfacial and gel properties of chickpea protein isolate, *LWT*, 2020, **129**, 109563.
 - 31 J. Resendiz-Vazquez, J. Urías-Silvas, J. Ulloa, P. Bautista-Rosales and J. Ramírez-Ramírez, Effect of ultrasound-assisted enzymolysis on jackfruit (*Artocarpus heterophyllus*) seed proteins: structural characteristics, technofunctional properties and the correlation to enzymolysis, *J. Food Process. Technol.*, 2019, **10**, 2.
 - 32 F. Jhan, A. Gani, N. Noor and A. Shah, Nanoreduction of Millet Proteins: Effect on Structural and Functional Properties, *ACS Food Sci. Technol.*, 2021, **1**, 1418–1427.
 - 33 Z. Zhu, W. Zhu, J. Yi, N. Liu, Y. Cao, J. Lu, E. A. Decker and D. J. McClements, Effects of sonication on the physicochemical and functional properties of walnut protein isolate, *Food Res. Int.*, 2018, **106**, 853–861.
 - 34 Z. Wei, Y. Wang, Z. Shi, N. Zhou, G. Ren, X. Hao, L. Zou and Y. Yao, Mung Bean Protein Suppresses Undernutrition-Induced Growth Deficits and Cognitive Dysfunction in Rats via Gut Microbiota-TLR4/NF-κB Pathway, *J. Agric. Food Chem.*, 2021, **69**(42), 12566–12577.
 - 35 J. L. Gehrig, S. Venkatesh, H. W. Chang, M. C. Hibberd, V. L. Kung, J. Cheng, R. Y. Chen, S. Subramanian, C. A. Cowardin, M. F. Meier, D. O'Donnell, M. Talcott, L. D. Spears, C. F. Semenkovich, B. Henrissat, R. J. Giannone, R. L. Hettich, O. Ilkayeva, M. Muehlbauer, C. B. Newgard, C. Sawyer, R. D. Head, D. A. Rodionov, A. A. Arzamasov, S. A. Leyn, A. L. Osterman, M. I. Hossain, M. Islam, N. Choudhury, S. A. Sarker, S. Huq, I. Mahmud, I. Mostafa, M. Mahfuz, M. J. Barratt, T. Ahmed and J. I. Gordon, Effects of microbiota-directed foods in gnotobiotic animals and undernourished children, *Science*, 2019, **365**, 169.
 - 36 I. H. Han, B. G. Swanson and B. K. Baik, Protein digestibility of selected legumes treated with ultrasound and high hydrostatic pressure during soaking, *Cereal Chem.*, 2007, **84**, 518–521.



- 37 G. Corsetti, C. Romano, E. Pasini, C. Testa and F. S. Dioguardi, Qualitative Nitrogen Malnutrition Damages Gut and Alters Microbiome in Adult Mice. A Preliminary Histopathological Study, *Nutrients*, 2021, **13**, 1089.
- 38 B. W. Hu, H. M. Li and X. Q. Zhang, A Balanced Act: The Effects of GH-GHR-IGF1 Axis on Mitochondrial Function, *Front. Cell Dev. Biol.*, 2021, **9**, 630248.
- 39 R. Schuler, M. Markova, M. A. Osterhoff, A. Arafat, O. Pivovarova, J. Machann, J. Hierholzer, S. Hornemann, S. Rohn and A. F. H. Pfeiffer, Similar dietary regulation of IGF-1-and IGF-binding proteins by animal and plant protein in subjects with type 2 diabetes, *Eur. J. Nutr.*, 2021, **60**(6), 3499–3504.
- 40 T. Wahyuni, A. Kobayashi, S. Tanaka, Y. Miyake, A. Yamamoto, A. Bahtiar, M. Kotaro, M. Maeda, M. Obana and Y. Fujio, Maresin 1 Induces Cardiomyocyte Hypertrophy Through ROR alpha/IGF-1/PI3K/Akt Pathway, *Circulation*, 2020, **142**, A14951.
- 41 M. Schwarzer, K. Makki, G. Storelli, I. Machuca-Gayet, D. Srutkova, P. Hermanova, M. E. Martino, S. Balmand, T. Hudcovic, A. Heddi, J. Rieusset, H. Kozakova, H. Vidal and F. Leulier, *Lactobacillus plantarum* strain maintains growth of infant mice during chronic undernutrition, *Science*, 2016, **351**, 854–857.
- 42 S. M. R. Camargo, R. N. Vuille-dit-Bille, C. F. Meier and F. Verrey, ACE2 and gut amino acid transport, *Clin. Sci.*, 2020, **134**, 2823–2833.
- 43 J. Torres, L. S. Munoz, M. Peters and C. A. Montoya, Heating and Soaking Influence in Vitro Hindgut Fermentation of Tropical Legume Grains in Pigs, *J. Agric. Food Chem.*, 2018, **66**, 532–539.
- 44 Y. S. Han, Q. Y. Zhao, C. H. Tang, Y. Li, K. Zhang, F. D. Li and J. M. Zhang, Butyrate Mitigates Weanling Piglets From Lipopolysaccharide-Induced Colitis by Regulating Microbiota and Energy Metabolism of the Gut-Liver Axis, *Front. Microbiol.*, 2020, **11**, 588666.
- 45 A. S. Raman, J. L. Gehrig, S. Venkatesh, H.-W. Chang, M. C. Hibberd, S. Subramanian, G. Kang, P. O. Bessong, A. A. M. Lima, M. N. Kosek, W. A. Petri, Jr., D. A. Rodionov, A. A. Arzamasov, S. A. Leyn, A. L. Osterman, S. Huq, I. Mostafa, M. Islam, M. Mahfuz, R. Haque, T. Ahmed, M. J. Barratt and J. I. Gordon, A sparse covarying unit that describes healthy and impaired human gut microbiota development, *Science*, 2019, **365**, 4735.
- 46 B. Byanju, M. M. Rahman, M. P. Hojilla-Evangelista and B. P. Lamsal, Effect of high-power sonication pretreatment on extraction and some physicochemical properties of proteins from chickpea, kidney bean, and soybean, *Int. J. Biol. Macromol.*, 2020, **145**, 712–721.
- 47 X. M. Hu, H. Y. Li, X. Y. Zhao, R. L. Zhou, H. H. Liu, Y. S. Sun, Y. Fan, Y. A. Shi, S. S. Qiao, S. J. Liu, H. W. Liu and S. Y. Zhang, Multi-omics study reveals that statin therapy is associated with restoration of gut microbiota homeostasis and improvement in outcomes in patients with acute coronary syndrome, *Theranostics*, 2021, **11**, 5778–5793.
- 48 M. Million, M. T. Alou, S. Khelaifia, D. Bachar, J. C. Lagier, N. Dione, S. Brah, P. Hugon, V. Lombard, F. Armougom, J. Fromonot, C. Robert, C. Michelle, A. Diallo, A. Fabre, R. Guieu, C. Sokhna, B. Henrissat, P. Parola and D. Raoult, Increased Gut Redox and Depletion of Anaerobic and Methanogenic Prokaryotes in Severe Acute Malnutrition, *Sci. Rep.*, 2016, **6**, 1–11.
- 49 R. Z. Hu, Z. Y. He, M. Liu, J. J. Tan, H. F. Zhang, D. X. Hou, J. H. He and S. S. Wu, Dietary protocatechuic acid ameliorates inflammation and up-regulates intestinal tight junction proteins by modulating gut microbiota in LPS-challenged piglets, *J. Anim. Sci. Biotechnol.*, 2020, **11**, 1–12.
- 50 Y. X. Liu, W. H. Li, H. X. Yang, X. Y. Zhang, W. X. Wang, S. T. Jia, B. B. Xiang, Y. Wang, L. Miao, H. Zhang, L. Wang, Y. J. Wang, J. X. Song, Y. J. Sun, L. J. Chai and X. X. Tian, Leveraging 16S rRNA Microbiome Sequencing Data to Identify Bacterial Signatures for Irritable Bowel Syndrome, *Front. Cell. Infect. Microbiol.*, 2021, **11**, 426.
- 51 D. Meng, W. S. Zhu, K. Ganguli, H. N. Shi and W. A. Walker, Anti-inflammatory effects of *Bifidobacterium longum* subsp *infantis* secretions on fetal human enterocytes are mediated by TLR-4 receptors, *Am. J. Physiol.: Gastrointest. Liver Physiol.*, 2016, **311**, G744–G753.
- 52 T. Requena, M. C. Martinez-Cuesta and C. Pelaez, Diet and microbiota linked in health and disease, *Food Funct.*, 2018, **9**, 688–704.
- 53 X. F. Zhou, B. W. Zhang, X. L. Zhao, Y. X. Lin, J. Wang, X. W. Wang, N. Hu and S. Wang, Chlorogenic acid supplementation ameliorates hyperuricemia, relieves renal inflammation, and modulates intestinal homeostasis, *Food Funct.*, 2021, **12**, 5637–5649.
- 54 W. T. Qu, X. J. Yuan, J. S. Zhao, Y. X. Zhang, J. Hu, J. W. Wang and J. X. Li, Dietary advanced glycation end products modify gut microbial composition and partially increase colon permeability in rats, *Mol. Nutr. Food Res.*, 2017, **61**, 1700118.
- 55 V. E. Wagner, N. Dey, J. Guruge, A. Hsiao, P. P. Ahern, N. P. Semenkovich, L. V. Blanton, J. Y. Cheng, N. Griffin, T. S. Stappenbeck, O. Ilkayeva, C. B. Newgard, W. Petri, R. Haque, T. Ahmed and J. I. Gordon, Effects of a gut pathobiont in a gnotobiotic mouse model of childhood undernutrition, *Sci. Transl. Med.*, 2016, **8**, 366ra164.
- 56 R. Y. Chen, I. Mostafa, M. C. Hibberd, S. Das, M. Mahfuz, N. N. Naila, M. M. Islam, S. Huq, M. A. Alam, M. U. Zaman, A. S. Raman, D. Webber, C. Zhou, V. Sundaresan, K. Ahsan, M. F. Meier, M. J. Barratt, T. Ahmed and J. I. Gordon, A Microbiota-Directed Food Intervention for Undernourished Children, *N. Engl. J. Med.*, 2021, **384**, 1517–1528.
- 57 S. Attia, C. J. Versloot, W. Voskuil, S. J. van Vliet, V. Di Giovanni, L. Zhang, S. Richardson, C. Bourdon, M. G. Netea, J. A. Berkley, P. F. van Rheenen and R. H. J. Bandstra, Mortality in children with complicated severe acute malnutrition is related to intestinal and systemic inflammation: an observational cohort study, *Am. J. Clin. Nutr.*, 2016, **104**, 1441–1449.

